JOURNAL OF MATERIALS SCIENCE 31 (1996) 1561–1567

The effect of the preparation method on the nature and dispersion of surface species formed upon reaction of molybdenum trioxide with alumina and titania

M. DEL ARCO, S.R.G. CARRAZÁN, C. MARTÍN, V. RIVES*
Departamento de Química Inorgánica, Universidad de Salamanca, Facultad de Farmacia. 37007-Salamanca, Spain

Titania- and alumina-supported molybdenum-containing systems have been prepared from mechanical mixtures of the support and molybdenum trioxide. The systems have been characterized by X-ray diffraction, temperature-programmed reduction and scanning electron microscopy, and Fourier transform–infrared monitoring of pyridine adsorption has been used to determine surface acidity. Dispersion of the supported phase, and its transformation to well-dispersed species has been attained by mechanical grinding and calcination in air, or by hydrothermal treatment of such mixtures and calcination. In the latter case, a higher dispersion is reached, despite the shorter time of calcination. Also hydrothermally treated samples show a larger concentration of surface Brönsted acid sites.

1. Introduction

Supported molybdenum trioxide is one of the most important heterogeneous catalysts (or catalyst components) because of its high activity in industrially relevant catalytic processes. In this context, MoO_3/Al_2O_3 systems are widely used as hydrotreatment catalysts, in processes such as hydrodesulphurization (HDS), hydrodenitrogenation (HDN) and hydrodemetallization (HDM) [1–3]. MoO_3/TiO_2 systems are used as effective catalysts for selective oxidation of propene, butene and methanol [4–6] and for reduction of NO with NH_3 [7]. Many studies have been carried out in order to analyse the behaviour of these catalysts in such processes and it has been shown that the activity and selectivity of these systems are modified by the nature and structure of surface molybdenum species [8, 9]. The formation of such surface species is strongly affected by variables such as preparation conditions, active phase components and the nature of the support [10]. In most cases, the best results have been obtained when the so-called monolayer catalysts are used, i.e. when the supported phase forms a single layer on the surface of the support.

From raster electron microscopy, Knözinger and Taglauer [11] concluded that the dispersion and size of molybdenum trioxide particles in MoO_3/Al_2O_3 systems prepared by mechanical mixing depends both on the grinding time and on the environment atmosphere during calcination. The nature of surface species obtained upon supporting molybdenum trioxide on silica, alumina and titania, in samples obtained by impregnation of all the three supports with heptamolybdate aqueous solutions, has been reported previously [12–14]. Samples have been also obtained by manually grinding mixtures of the oxide support and molybdenum trioxide [15–17], and we have reported the effect of calcination under different environmental conditions on the dispersion state of this type of solid. In the present paper, we report on MoO_3/Al_2O_3 and MoO_3/TiO_2 samples with different molybdenum trioxide loadings prepared by mechanically mixing the support and the supported oxide, but submitting the mixtures to hydrothermal treatment prior to calcination at high temperature, in order to analyse the formation of oxo-hydroxy-molybdenum species, the presence of which has been claimed to favour dispersion of molybdenum trioxide [13].

An investigation and comparison of the interaction of molybdenum trioxide with Al_2O_3 and TiO_2 support were attempted in this work. In particular, the work was focused on the phenomenon of spreading and the identification of the molybdenum-containing species formed on the support. X-ray diffraction (XRD) and temperature-programmed reduction (TPR) have been used to obtain information on the spreading of MoO_3 on these supports. These results are compared with previous laser Raman spectra (LRS) [18], in which different molybdenum species formed on these supports have been identified. Scanning electron microscopy (SEM) measurements have

*Author to whom all correspondence should be addressed.

0022–2461

been also carried out in order to obtain information about the morphology of the samples' surface.

2. Experimental procedure

2.1. Materials and samples preparation

The supports Al_2O_3 (γ-alumina, reference RV005, hereafter A) and TiO_2 (P-25, containing both anatase and rutile, hereafter T) were obtained from Degussa (Germany), and were calcined in air overnight at 770 K to eliminate adsorbed organic impurities.

Two series of samples were prepared on each support: samples belonging to series M and series H. Different amounts of MoO_3 (equivalent to 0.4–2 monolayers) were added to the supports and then they were manually ground for 20 min. A portion of these mixtures was calcined in static air atmosphere for 24 h in an open crucible at 773 K (series M). Another portion of the mixtures was suspended in water (1 g/25 ml) and hydrothermally treated at 423 K for 3 h in a PHAXE 2001 digestion bomb. These samples were dried at 373 K (samples H/373) and then calcined at 773 K for 3 h in air, as described above for M samples (samples H/773). Molybdenum loadings corresponded in all cases to 0.4, 0.7, 1, 1.5 and 2 monolayers, taking this as the amount of MoO_3 needed to cover geometrically the surface of the support, and calculated from the BET surface area of the supports ($S_{BET}Al_2O_3 = 105\ m^2\ g^{-1}$, $S_{BET}TiO_2 = 50\ m^2\ g^{-1}$) and the area occupied by a "molecule" of MoO_3, $15 \times 10^4\ pm^2$ [19]. In all cases, molybdenum trioxide loading is given as a figure indicating the number of monolayers.

2.2. Experimental techniques

XRD patterns were obtained by reflection from powder packed in a sample holder with a Siemens-500 diffractometer using $CuK_{\alpha 1}$ radiation ($\lambda = 154.05$ pm) equipped with a graphite monochromator and interfaced to a DACO-MP data acquisition microprocessor.

TPR profiles were recorded in a Micromeritics TPR/TPD 2900 apparatus, using a 5% H_2–Ar mixture as carrier gas (from Sociedad Española del Oxígeno, SEO, Spain), with a flow of 50 ml min^{-1} and a heating rate of 10 K min^{-1} up to 1170 K, this temperature being maintained for 30 min. The amount of sample (containing ~90 mmol MoO_3) was chosen taking into account the molybdenum loading, the heating rate and the gas flow, in order to ensure good resolution of the reduction peaks under the experimental conditions used [20].

SEM images of samples were obtained with a Zeiss DSM 940 digital scanning microscope between 20 and 30 kV with magnifications between 1.000 and 10.000. The maximum resolution was 5 nm at 30 kV. Samples were sputtered with gold for 150 s using a BIO-RAD-SEM loading, working at 1.6 kV and 25 mA.

Adsorption of pyridine (py, from Fluka) for surface acidity assessment, was monitored by Fourier transform–infrared (FT–IR) spectroscopy, using a Perkin–Elmer PC-16 spectrometer, connected to an Ataio 386-SX computer, using special cells with CaF_2 windows. Nominal resolution was 2 cm^{-1}, and 100 runs were averaged to improve the signal-to-noise ratio. Samples were submitted *in situ* to a conditioning treatment, consisting in outgassing at 670 K for 2 h (residual pressure $10^{-3}\ N\ m^{-2}$). After equilibration with a small pyridine pressure, the spectrum was recorded after outgassing at temperatures ranging from room temperature to 673 K. In all cases, the spectrum of the solid was substracted using the capabilities provided by the computer software.

3. Results and discussion

3.1. Mechanical mixtures (samples M)

Dispersion of the surface molybdenum-containing species in MT samples was determined from quantitative XRD measurements of the residual crystalline MoO_3 phase in these samples, calculated from the area of the XRD MoO_3 peak at 381 pm, because the strongest MoO_3 peak at 326 pm overlaps with the main diffraction peak of anatase.

A plot of the residual amount of crystalline MoO_3 versus the total amount of MoO_3, as determined by XRD, for samples obtained on the titania support, is shown in Fig. 1; results corresponding to the MA samples [15] are also included for comparing both systems. There is a threshold at 0.056 g MoO_3/g TiO_2. When the total amount of MoO_3 is lower than this value, no MoO_3 peak was detected. On the other hand, the surplus of MoO_3 increases linearly with the total amount of MoO_3. Taking into account the specific surface area of TiO_2, the dispersion capacity corresponds to 0.11 g MoO_3/100 m^2 TiO_2. In the case of MoO_3/Al_2O_3 samples, the threshold is at 0.126 g MoO_3/g γ-Al_2O_3, which corresponds to a dispersion capacity of 0.12 g MoO_3/100 m^2 γ-Al_2O_3 [15]. Similar values have been reported by Xie *et al.* [21] for MoO_3/Al_2O_3 samples (0.12 g MoO_3/100 m^2 support) prepared by mechanical mixing of molybdenum trioxide and the supports, despite the specific surface area of the supports used by these authors being larger

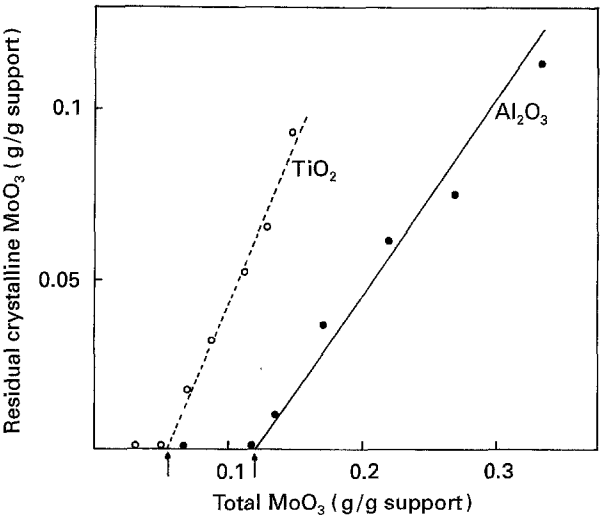

Figure 1 Amount of residual crystalline MoO_3 versus total amount of MoO_3 in samples MA and MT.

than those used in the present study (178 $m^2 g^{-1}$ for Al_2O_3).

From the above results it can be concluded that the experimental MoO_3 dispersion capacity corresponds to 1.4 monolayers in the case of the MT system, compared to 0.72 monolayers for the MA samples. In other words, molybdenum trioxide loadings below these threshold values result in total dispersion (at least, at the detection level provided by X-ray diffraction).

Also, the values determined for the highest dispersion capacities are in good agreement with those calculated assuming that the active component, MoO_3, forms a close packed monolayer on the surface of γ-Al_2O_3 and TiO_2; in such a case, the monolayer coverage corresponds to 0.12 g MoO_3/100 m^2 of support. On the basis of these results, it can be concluded that the highest dispersion capacity of MoO_3 on Al_2O_3 and TiO_2 is the same for both supports. The value of 0.12 g MoO_3/100 m^2 γ-Al_2O_3 (0.72 theoretical monolayers) for the highest dispersion capacity in samples MA calcined 24 h in air, obtained by XRD, coincides, within experimental error, with that found by zero-point-charge (ZPC) measurements (0.8 monolayers) [16]. Thus, for MA samples calcined for 24 h, we concluded that the surface of the support is completely covered when the molybdenum trioxide loading is about 0.7–0.8 monolayers. Unfortunately, no ZPC results are available for MT systems. Thus, the results obtained by XRD for MT samples only indicate that no MoO_3 peak is recorded for loadings below 1.4 monolayers, while peaks due to bulk MoO_3 are recorded for loadings of about 0.7–0.8 monolayers for samples MA. These results suggest that the spreading of molybdenum trioxide on the titania surface is easier than on the alumina surface.

Dispersion of the supported phase has been also analysed by electron microscopy. Micrographs for MA samples have been reported previously [15]. A bimodal distribution of particle shapes is observed in Fig. 2 for sample MT2; molybdenum trioxide appears as elongated platelets, while the aggregates correspond to the support TiO_2. For MT0.7 sample, only aggregates have been recorded. Taking into account that all samples were prepared in a similar way (only differing in the molybdenum trioxide loading within each series), it should be concluded that the lack of elongated particles in sample MT0.7 should be due to total dispersion of molybdenum trioxide, while its presence in sample MT2 should be ascribed to the fact that in this sample the maximum dispersion capacity has been surpassed.

The nature of the molybdenum-containing species existing in the different systems studied has been determined by laser Raman spectroscopy [18, 22]; in all cases, total transformation of MoO_3 into dispersed polymolybdate species for samples MA and into mono-oxo-molybdenum species (with a single $Mo{=}O_{terminal}$ moiety) for samples MT, has been observed, such a transformation being favoured by the presence of water vapour during calcination.

The nature and dispersion degree of the molybdenum-containing species in samples MA and MT can also be assessed from its reducibility. This is a very important property, as these systems also find application in selective oxidation processes, where they undergo red-ox transformation, the ease of which will depend on its reducibility degree. The temperature-programmed reduction (TPR) of these samples is reported. Hydrogen consumptions (expressed as the ratio between the molecules of hydrogen consumed, against the number of atoms of molybdenum in the samples) are given in Table I. A value of 3.0 would be expected in all cases, corresponding to reaction

$$Mo^{VI} + 3H_2 \rightarrow Mo^0 + 6H^+ \quad (1)$$

i.e. total reduction of Mo^{VI} to the metallic state.

Samples MA show TPR profiles [16] with a sharp, intense maximum at 723 K that shifts towards 750 K as the molybdenum content is increased, and that has been ascribed to reduction of polymolybdate species; as the molybdenum content is further increased, reduction peaks are also recorded at higher temperatures, which have been ascribed to reduction of dispersed molybdenum trioxide (at 920 K) and bulk molybdenum trioxide (at 1100 K) [16].

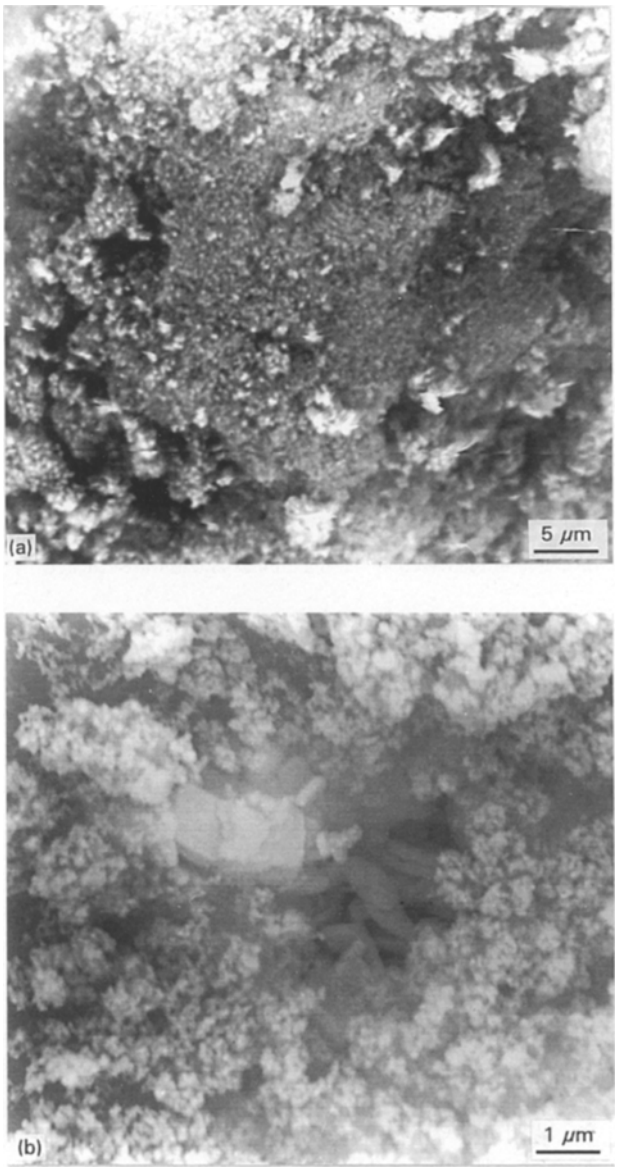

Figure 2 Scanning electron micrographs of (a) MT0.7 and (b) MT2.

TABLE I Hydrogen consumption during temperature-programmed reduction analysis of the samples studied

Sample	H_2/Mo ratio[a]		
	Total	1st peak	2nd peak
MT0.5	3.02	1.56	1.56
MT0.7	3.01	1.55	1.56
MT1	2.98	1.50	1.48
HA0.7/373[b]	2.22	0.98	1.24
HA1/373[b]	2.30	0.99	1.31
HA0.7/773[b]	2.54	0.94	1.60
HA1/773[b]	2.28	0.98	1.30
HT0.7/373	2.36	1.61	0.75
HT1/373	2.12	1.08	1.04
HT0.7/773	2.61	1.63	0.98
HT1/773	2.61	1.55	1.06

[a] Mol H_2/ at Mo.
[b] Base line unrecovered at the maximum temperature reached.

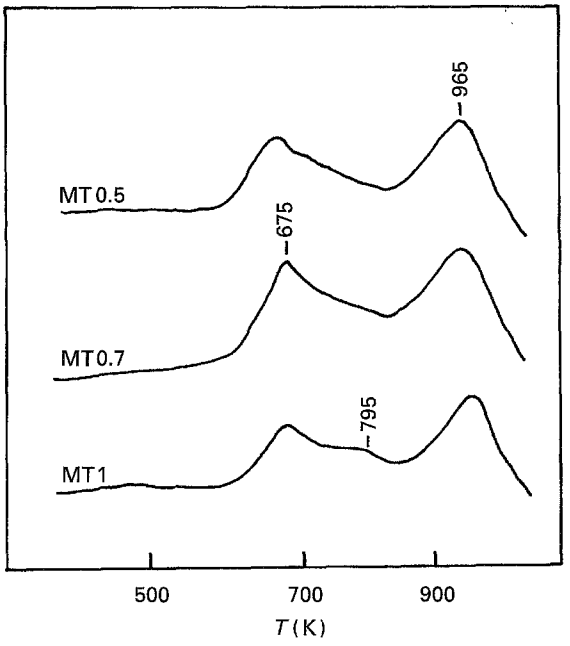

Figure 3 TPR profiles of samples MT0.5, MT0.7 and MT1.

Reduction profiles for samples MT are given in Fig. 3. They all show two maxima, at 675 and 965 K, although a third peak, recorded as a shoulder at 795 K, is recorded, in addition, for the high-loaded sample, MT1. Taking into account the conclusions drawn from the XRD study described above, the peaks at 675 and 965 K correspond to reduction of dispersed mono-oxomolybdenum species, identified by laser Raman spectroscopy [18]. In MoO_3/TiO_2 samples with the same loadings as those in the samples studied here, but prepared by impregnation of titania with aqueous solutions of ammonium heptamolybdate, two reduction maxima were recorded at 750 and 1040 K [14], i.e. about 75 K higher. For these samples, LRS indicates the formation of polymolybdate species. The shoulder at 795 K in the reduction profile of sample MT1 can be tentatively ascribed to the presence of highly dispersed molybdena, undetected by XRD, the reduction profile of which, in samples obtained by impregnation, is recorded at 885 K. The amount of hydrogen consumed corresponds to 3.0 ± 0.2 mol H_2/ at Mo, Table I. The areas of the two peaks recorded correspond to an average of 1.5 and 1.5 mol H_2/ at Mo for the first and second peaks, respectively. If a step-by-step reduction is assumed, these values would correspond to a two-step process, $Mo^{VI} \rightarrow M^{III} \rightarrow Mo^0$. However, this could not be checked, as the reduction could not be stopped after the first reduction peak and before the second one, and so the actual oxidation state of molybdenum after the first reduction peak is unknown at the moment.

3.2. Hydrothermally prepared samples

Hydrothermally treated samples were dried at 373 K and then calcined in an open crucible at 773 K; however, in this case calcination was only for 3 h, whereas the samples obtained by mechanical mixing were calcined for 24 h. All studies were performed for both sets (dried at 373 K and calcined at 773 K), in order to ascertain if the hydrothermal treatment (hereafter HTT) favoured the formation of oxohydroxy-molybdenum species, which in turn increase molybdenum dispersion [23–25].

XRD diagrams for samples HT/373 and HT/773 do not exhibit any diffraction peak due to molybdenum-containing species for molybdenum loadings lower than 1.4 monolayers of MoO_3; for higher loadings, a peak is recorded at 381 pm, the intensity and half-width for which indicate that it corresponds to bulk molybdenum trioxide.

Thus, it can be concluded that HTT of MoO_3–TiO_2 mixtures leads to total dispersion of molybdenum-containing species for loadings lower than that equivalent to 1.4 monolayers of MoO_3, and no further calcination increases the maximum dispersion capability. Such a limiting value for dispersion coincides with that attained for the mechanical mixtures (samples MT), after being calcined in an open crucible for 24 h. Therefore, it should be concluded that the key factor for molybdenum dispersion on titania should be the contact with water.

The behaviour shown by samples HA is rather different, as dispersion (at least, from the XRD point of view) depends on the calcination temperature, as well as the molybdenum loading, Fig. 4. No MoO_3 peak is therefore recorded for sample HA0.7. For samples HA1/373 and HA1.5/373 (i.e. those containing 1 and 1.5 monolayers of MoO_3, respectively, and calcined at 373 after HTT), weak peaks are recorded in positions close to those of bulk molybdenum trioxide, which have been ascribed [26] to hydrated oxides, $MoO_x \cdot nH_2O$. When these samples are calcined at 773 K, peaks similar to those of bulk molybdenum trioxide are recorded, although at spacing values slightly higher, the peaks at 313 and 308 pm (previously ascribed to hydrated oxides) now being absent. The shift observed and the changes in half-width could originate from a lack of crystallinity of the MoO_3 species. Peaks coincident (with respect to position and halfwidth) with those of molybdenum trioxide are

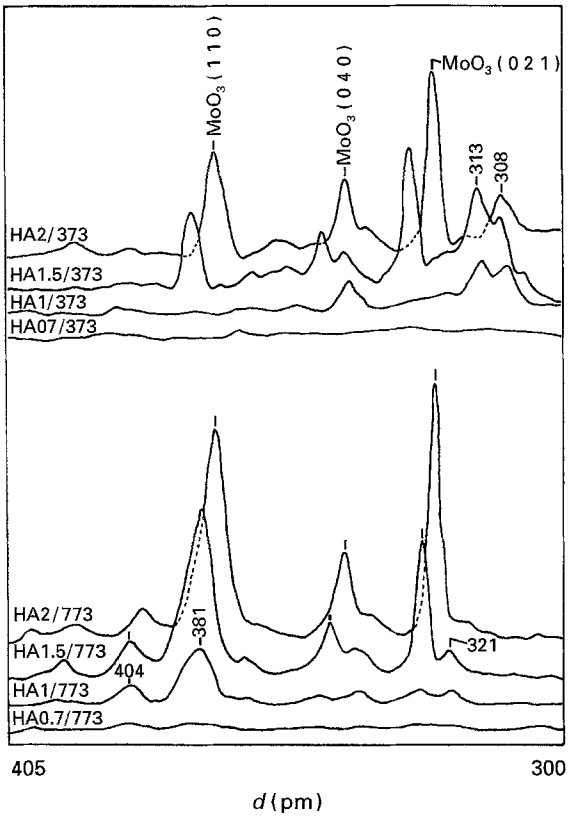

Figure 4 XRD profiles of the samples HA/373 and HA/773.

recorded for samples HA2, both before and after calcination at 773 K. As the maximum dispersion limit has been surpassed in these samples, it should be concluded that these peaks correspond to bulk MoO_3.

The existence of bulk molybdenum trioxide in HTT samples and MoO_3 loadings exceeding the maximum dispersion limit, can also be concluded from the SEM studies. The micrographs in Fig. 5 correspond to samples HT1.5 and HA1.5 calcined at 773 K; for lower loadings, only aggregates (i.e. support particles) are seen, while in these cases (when the dispersion capability has been surpassed), a bimodal distribution of particles (elongated platelets, in addition to aggregates) is observed.

LRS studies [18] have shown spectra similar to that of heptamolybdate for samples HA/373 (i.e. HTT, uncalcined), thus indicating that molybdenum trioxide transformation to heptamolybdate takes place in the presence of water; MoO_3 exists in sample HA0.7/773, where polymolybdates are not recorded (probably due to their very low concentration), while for higher loadings the simultaneous presence of MoO_3 and polymolybdates is found.

On the other hand, the LR spectra of samples HT/373 show a band at 970 cm^{-1}, due to polymolybdate species, which disappears after calcination at 773 K, while another band develops at 994 cm^{-1}, due to mono-oxo-molybdenum species [18].

TPR profiles for samples HA are included in Fig. 6a. In all cases, a sharp peak similar to that recorded for samples MA, is recorded at 725 K. This peak should be ascribed to reduction of heptamolybdate species, the presence of which has been confirmed by LRS. Calcination of sample HA0.7 at 773 K leads

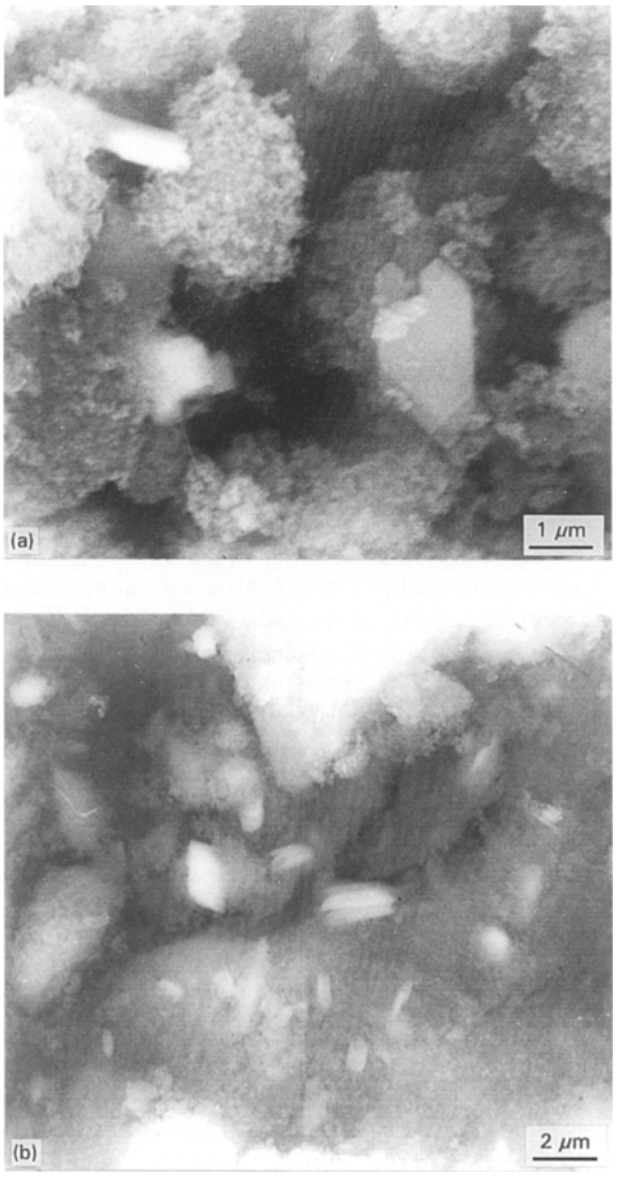

Figure 5 Scanning electron micrographs of (a) HT1.5/773 and (b) HA1.5/773.

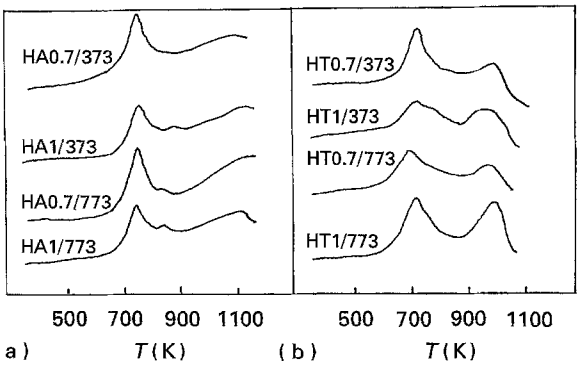

Figure 6 TPR profiles of samples (a) HA and (b) HT.

to the presence of a weak, new reduction peak at 850 K that can be tentatively ascribed to reduction of dispersed MoO_3, the presence of which has also been confirmed by LRS.

Similar spectra are recorded for samples HA1, although, owing to the larger molybdenum content,

a weak peak, due to reduction of dispersed molybdenum oxide, is recorded at 850 K, and is confirmed by LRS. No peak due to reduction of bulk MoO_3 is recorded in any case.

No firm quantification of these data can be made, as the curve recorded does not recover to the base line, even at the maximum temperature reached in our experimental system, i.e. total reduction requires a larger amount of hydrogen than that recorded. Even so, the first reduction peak corresponds to ~ 1 mol H_2/at Mo, and so it could be claimed that such a first reduction corresponds to the $Mo^{VI} \rightarrow Mo^{IV}$ process, although this could not be confirmed.

Reduction profiles for samples HT, Fig. 6b, are similar to those for samples MT. However, the peaks are recorded at slightly higher temperatures (710–720 and 1000 K). Nevertheless, the positions of these peaks are between those reported for mono-oxo-molybdates and polymolybdates [14, 27]. Although in these cases the curves recover to the base line before the maximum temperature is reached, total hydrogen consumption is slightly lower than the amount required for total reduction of molybdenum to the metallic state.

In order to complete the characterization of these samples, its surface acidity has been assessed by FT–IR monitoring of pyridine (py) adsorption. Changes in surface acidity become important in catalytic reactions where dehydration takes place.

The spectra recorded were rather similar in all cases. Those for samples HA1.5/773 and HT1.5/773 are shown in Fig. 7. For sample HA1.5/773, Fig. 7a, two bands at 1609 and 1448 cm^{-1} (modes 8a and 19b) are due to pyridine coordinated to surface Lewis sites, while those at 1638 and 1538 cm^{-1} are due to the pyridinium ion, i.e. both surface Lewis sites and Brönsted sites exist in this sample. The latter are absent in the parent support, and thus develop upon molybdenum incorporation. Desorption at increasing temperatures leads to a slight decrease of the bands, but they remain even after outgassing at 673 K, thus indicating that surface sites are strongly acidic.

A similar behaviour is observed for sample HT1.5/773, the corresponding spectra being included in Fig. 7b. The bands originated by pyridine coordinatively bonded to surface Lewis acid sites are recorded at 1608 and 1447 cm^{-1}, while the presence of Brönsted sites (absent in the surface of titania) is confirmed by the bands at 1638 and 1537 cm^{-1}, due to pyridinium ions. Again, outgassing at increasing temperatures only slightly decreases the intensities of these bands, which remain even after outgassing at 673 K, thus indicating that sites responsible for adsorption are strongly acidic.

The relative amounts of Brönsted and Lewis acid sites can be determined from the ratio between the intensities (areas) of the peaks due to mode 19b of pyridinium ion and coordinated pyridine. Such ratios are larger than those calculated for samples similar to those here studied, but prepared by impregnation [28]. In the present case, the values are always larger than one. This finding indicates that a larger concentration of surface Brönsted acid sites develop by

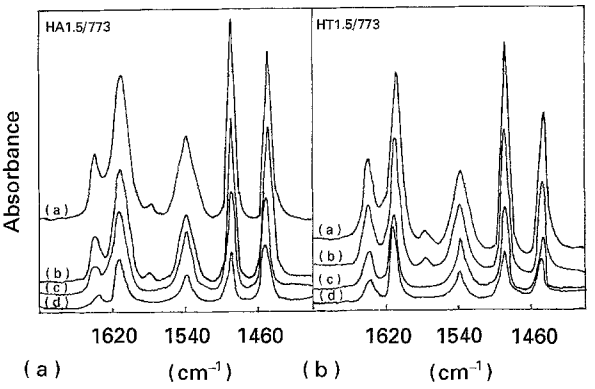

Figure 7 FT–IR spectra of pyridine absorbed on samples HA1.5/773 and HT1.5/773 outgassed at (a) 373, (b) 473, (c) 573 and (d) 673 K.

hydrothermal treatment than by impregnation from aqueous solutions or mere calcination of mechanical mixtures of both oxides (once the loading has surpassed that corresponding to a monolayer). This is in agreement with the larger molybdenum dispersion in the samples studied here, as detected by XRD and LRS; moreover, Miyata *et al.* [29] have reported that two-dimensional or monolayer species are stronger Brönsted acids than those obtained with large molybdenum loadings.

4. Conclusion

From the results described for hydrothermally treated mixtures (molybdena and alumina, or molybdena and titania) it is concluded that the nature of the surface species formed, and the dispersion degree attained, are in all cases rather similar to those obtained by calcining mechanical mixtures for a longer period of time; however, the hydrothermal treatment seems to be more convenient, as energy consumption during this treatment and short-term calcination is lower than during prolonged calcination to attain the same dispersion level.

Acknowledgements

Financial support from the Ministerio de Educación y Ciencia (Madrid, Spain, ref. PB91-0425 and PB93-0633) is acknowledged. Mr A. Montero is thanked for his assistance in TPR measurements.

References

1. T. I. YANG and L. H. LUNSFORD, *J. Catal.* **63** (1980) 505.
2. H. F. LIU, R. S. LIU, K. I. LIEW, R. E. JOHNSON and L. H. LUNSFORD, *J. Am. Chem. Soc.* **106** (1982) 4117.
3. J. ABART, E. DELGADO, G. ESST, H. JEZIOROWSKI, H. KNOZINGER, N. THIELE, X. Z. H. WANG and E. TAGLAUER, *Appl. Catal.* **2** (1982) 155.
4. D. VANHOVE, S. R. OP, A. FERNANDEZ and M. BLANCHAR, *J. Catal.* **57** (1979) 253.
5. T. ONO, Y. NAKAGAWA, H. MIYATA and Y. KUBOKAWA, *Bull. Chem. Soc. Jpn.* **57** (1984) 1205.
6. J. C. VOLTA and J. L. PORTEFAIX, *Appl. Catal.* **18** (1985) 32.

7. S. OKAZAKI, M. KUMASARA, J. YOSHIDA, K. KOSAKA and K. TANABE, *Ind. Eng. Chem. Prod. Res. Dev.* **20** (1981) 301.
8. H. KNOZINGER, in "Proceedings of the 9th International Congress on Catalysis", Vol. 5, edited by M. J. Phillips and M. Ternan (Chemical Institute of Canada, Calgary, 1988) p. 20.
9. S. R. STAMPFT, Y. CHEN, J. A. DUMESIC, C. H. NIU and C. G. HILI, *J. Catal.* **105** (1985) 445.
10. H. JEZIOROWSKI and H. KNOZINGER, *J. Phys. Chem.* **83** (1976) 116.
11. H. KNOZINGER and E. TAGLAUER, in "Catalysis, Specialist Periodical Report", J. J. Spivey and S. K. Agarwal (Snr. Reps.) Vol. 10, (Royal Society of Chemistry, Cambridge, 1993). p. 1.
12. M. DEL ARCO, M. J. HOLGADO, C. MARTIN and V. RIVES, *Langmuir* **6** (1990) 801.
13. M. DEL ARCO, C. MARTIN, V. RIVES, V. SÁNCHEZ ESCRIBANO, G. RAMIS, G. BUSCA, V. LORENZELLI, P. MALET, *J. Chem. Soc. Farad. Trans.* **89** (1993) 1071.
14. M. DEL ARCO, S. R. G. CARRAZAN, I. MARTIN, C. MARTIN, V. RIVES and P. MALET, *J. Mater. Chem.* **5** (1993) 1313.
15. M. DEL ARCO, S. R. G. CARRAZAN, V. RIVES and J. V. GARCIA RAMOS, *Mater. Chem. Phys.* **31** (1992) 202.
16. M. DEL ARCO, S. R. G. CARRAZAN, V. RIVES, F. J. GIL-LLAMBIAS and P. MALET, *J. Catal.* **141** (1993) 48.
17. M. DEL ARCO, S. R. G. CARRAZAN, V. RIVES and P. MALET, *J. Mater. Sci.* **29** (1994) 2309.
18. M. DEL ARCO, S. R. G. CARRAZAN, C. MARTIN, V. RIVES, J. V. GARCIA RAMOS and P. CARMONA, *Spectrochim. Acta* **50A** (1994) 2215.
19. T. FRANSEN, P. C. VAN BERGE and P. MARS, in "Preparation of Catalysts", Vol. 1, edited by B. Delmon, P. A. Jacobs and G. Poncelet, (Elsevier, Amsterdam, 1975) p. 405.
20. P. MALET and A. CABALLERO, *J. Chem. Soc. Farad. Trans. I* **84** (1988) 2369.
21. Y. XIE, L. GUI, Y. LUI, B. ZHAO, N. YANG, Y. ZHANG, Q. GUO, L. ZUAN, H. HUANG, X. CAI and Y. TANG, in "Adsoption and Catalysis on Oxide Surfaces", edited by M. Che and G. C. Bond, (Elsevier, Amsterdam, 1985) p. 139.
22. M. DEL ARCO, S. R. G. CARRAZAN, V. RIVES and J. V. GARCIA RAMOS, *Spectrosc. Lett.* **25** (1992) 73.
23. O. GLEMSER and H. G. WENDLAND, *Angew. Chem.* **75** (1963) 949.
24. *Idem, Adv. Inorg. Chem. Radiochem.* **5** (1963) 215.
25. O. GLEMSER and R. HAESELER, *Z. Anorg. Allgem. Chem.* **316** (1962) 168.
26. Joint Committee on Powder Diffraction Standards (International Centre for Diffraction Data, Pennsylvania, USA, 1971).
27. C. MARTÍN, I. MARTÍN, V. RIVES and P. MALET, *J. Catal.* **147** (1994) 465.
28. M. DEL ARCO, S. R. G. CARRAZÁN, C. MARTÍN, I. MARTÍN and V. RIVES, *Spectrochim. Acta* **50A** (1994) 697.
29. H. MIYATA, K. FUJI and T. ONO, *J. Chem. Soc. Farad. Trans. I* **84** (1988) 3121.

Received 14 June 1994
and accepted 8 September 1995